GEOPHYSICAL RESEARCH LETTERS,VOL. 22, NO. 6, PAGES 731-734, MARCH 15, 1995

SH-wave propagation in the whole mantle using high-order finite differences

Heiner Igel

Institute of Theoretical Geophysics, Cambridge, UK

Michael Weber

Institut für Geophysik, Göttingen, Germany

Abstract. Finite-difference approximations to the wave equation in spherical coordinates are used to calculate synthetic seismograms for global Earth models. High-order finite-difference (FD) schemes were employed to obtain accurate waveforms and arrival times. Application to SH-wave propagation in the mantle shows that multiple reflections from the core-mantle boundary (CMB), with travel times of about one hour, can be modeled successfully. FD techniques, which are applicable in generally heterogeneous media, can be used to determine realistic global earth structure.

Introduction

Lateral heterogeneities in the Earth have considerable effects on the arrival times and waveforms recorded at the Earth's surface. These effects can not be modeled by techniques based on the assumptions of spherical symmetry such as the reflectivity method [*Fuchs and Müller, 1971*] or normal modes [see e.g. *Woodhouse and Dziewonski, 1984*, *Wysession and Shore, 1994*], where only small perturbations about a reference model can be treated. High frequency approximations [see e.g. *Červený et al., 1982*] are not adequate in strongly inhomogeneous media. The Direct Solution Method [*Geller and Ohminato, 1994*, *Cummins et al., 1994a,b*], a solution of the weak form of the wave equation for heterogeneous media, has been applied to global seismology but not yet to models with strong lateral heterogeneities.

The FD technique [see e.g. *Alterman et al., 1970*, *Virieux, 1986*, *Chaljub et al., 1995*] has the advantage that wave propagation can be simulated by directly solving the equation of motion for arbitrary heterogeneous models. One drawback of this technique, however, is that it requires enormous computational resources.

Recently, the new generation of massively parallel hardware has led to an increasing number of applications of FD techniques to seismic wave propagation in 2D and 3D media [*Rodrigues and Mora, 1992*; *Igel et al., 1993*].

In this study, the second-order scheme based on a staggered-grid formulation [*Chaljub et al., 1995*] is extended to higher orders considering toroidal motion (SH-waves) in 2D. This leads to considerably improved accuracy in travel time and waveform.

Paper number 95GL00204
0094-8534/95/95GL-00204$03.00

Theory

In a spherical coordinate system with coordinates $\{r, \varphi, \theta\}$ — assuming invariance in φ for all fields — the equation for toroidal motion u^φ (SH-waves) is

$$\rho \frac{\partial^2 u^\varphi}{\partial t^2} = f^\varphi + \frac{1}{r^4}\frac{\partial (r^4 \sigma_r{}^\varphi)}{\partial r} + \frac{1}{r^2 \sin^3\theta}\frac{\partial ((\sin^3\theta)\, \sigma_\theta{}^\varphi)}{\partial \theta}, \tag{1}$$

where ρ is the mass density, f^φ is a volumetric force, $\sigma_i{}^j$ are the components of the stress tensor,

$$\sigma_r{}^\varphi = \mu \frac{\partial u^\varphi}{\partial r}, \qquad \sigma_\theta{}^\varphi = \mu \frac{\partial u^\varphi}{\partial \theta}, \tag{2}$$

μ being the shear modulus. Sources and inhomogeneities are invariant in φ–direction.

Wave motion is simulated between the Earth's surface and the CMB. These boundaries can be approximated by a free surface boundary condition, where $\sigma_r{}^\varphi = 0$.

Finite-difference approximation

FD approximations of space derivatives can be expressed as a convolution sum [see e.g. *Rodrigues and Mora, 1992*], where the number of adjacent grid values used to calculate the derivative determines its accuracy. The weights for derivative operators of different length can be obtained analytically [see e.g. *Igel et al.*, 1993]. Convolution-based FD operators are particularly suited to massively parallel computers since they use the fast communication between neighbor processors.

The fields are defined on a staggered grid. In staggered grid methods, the derivative of a discrete field is calculated halfway between the grid points where the field is defined [*Virieux*, 1986]. This implies that u^φ

and $\sigma_r{}^\varphi$, $\sigma_\theta{}^\varphi$ of equations (1) and (2) respectively are defined at different locations. Such a scheme converges faster and results in improved accuracy [*Viricux*, 1986].

Due to the singularity of the coordinate system at θ=0° the source is located at the grid point closest to the axis, and the displacement component is kept constant $u^\varphi = 0$ at θ=0° and 180° from symmetry considerations.

The displacement field u^φ is extrapolated in time using a Taylor's expansion

$$u^\varphi(t+\Delta t) = 2u^\varphi(t) - u^\varphi(t-\Delta t) + 2\sum_{n=1}^{N} \frac{\Delta t^{2n}}{(2n)!} u^{\varphi(2n)}(t), \quad (3)$$

where Δt is the time increment and N is the order of the time extrapolation. Note that the high-order time derivatives $u^{\varphi(2n)}$ can be obtained by repeatedly looping through the algorithm [*Igel et al.*, 1993]. Stability and dispersion for the cartesian version of such an algorithm has been studied by *Rodrigues and Mora* [1992].

Simulation Example

In a feasibility test we apply this algorithm to the PREM model [*Dziewonski and Anderson*, 1981] without absorption. The model is defined on a 4096 x 1000 grid with an angular range of 180° and a maximum depth of 2891km. This results in a depth spacing of $\approx$ 2.9km and an angular spacing (arc length) between $\approx$ 4.9km (at the surface) and $\approx$ 2.7km (at the CMB). The time increment is 0.15 s and 24000 time steps are propagated (total recording time of one hour). A simulation with an eight-point operator in space (see *Igel et al.* [1993] for the cartesian case) and N=4 in time (Eq. 3) requires 150 minutes CPU on a 128-processor Connection Machine CM-5 including I/O.

Figure 1 shows snapshots of SH-waves. The source time function is the first derivative of a Gaussian with a dominant period of $\approx$40 s and a cutoff at $\approx$10 s. Fundamental properties of SH-waves reverberating in the mantle can be observed [see also *Shearer, 1991; Wysession and Shore, 1994*]: (1) SH-waves reflected by the CMB reach the surface with a curvature slightly stronger than the curvature of the Earth's surface and are thus reflected back as nearly *planar* features (Fig-

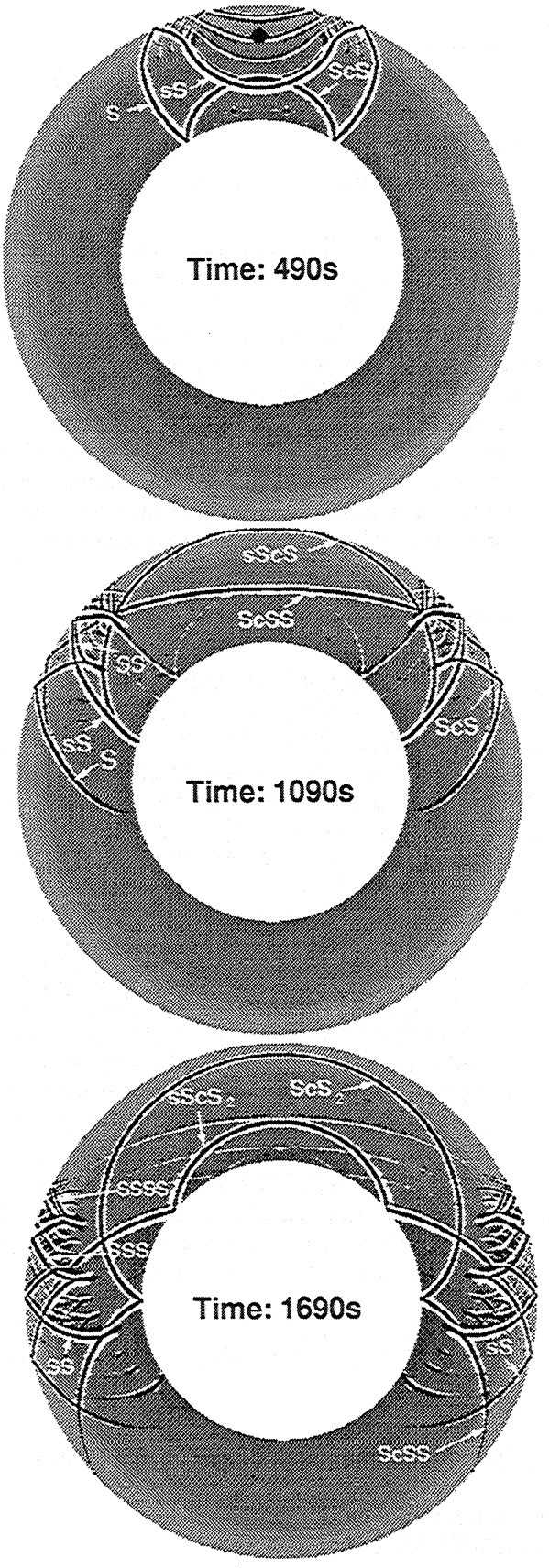

Figure 1. SH-wave snapshots. The source is at 640km depth. The borders of the model are the free surface and the CMB respectively. The grey shading is relative to the S-velocity (PREM). Black and white denote positive and negative displacement, respectively. All amplitudes above 0.1% of the maximum amplitude in the snapshot are shown. Top: After 490 s. The source location is indicated by a dot. Downgoing S has been reflected at the CMB (ScS). Upgoing S has been reflected by the Earth's surface (sS). Middle: After 1090 s. sS trails S by about 17° at the surface. $sScS$ reaches the Earth's surface. Bottom: After 1690 s. sS has reached a distance of 102° at the surface, i.e. its ray-theoretical core shadow boundary. Note the amplitude decay of the wavefront still in the mantle. ScS_2 is about to reach the surface and is trailed by $sScS_2$.

ure 1, 1090 s, $ScSS$). (2) The upper mantle discontinuities produce a train of phases trailing the main phases (see e.g. Figure 1, 490 s). (3) Multiple S reflections from the surface lead to an increasing number of Y-shaped wavefronts (Figure 1, 1090 s and 1690 s). (4) The wavefield propagating along the surface becomes increasingly complex due to internal reverberations in the upper mantle and multiple surface reflections (Figure 1, 1690 s).

The corresponding seismograms for epicentral distances up to 125° are shown in Figure 2. Note that phases such as $sScS_3$, observed at around 100° epicentral distance, have propagated more than 100 wavelengths.

Numerical Dispersion

Numerical dispersion may alter the travel time and lead to a distortion of the propagating pulse similar to the effects of physical dispersion. In order to estimate the numerical dispersion of this scheme, waves are propagated through a homogeneous mantle model (v_s=6.5km/s) and PREM for a source depth of 640km. The grid parameters are the same as described above; the dominant period of the source function is 25 seconds. The results are shown in Figure 3. For both models, seismograms for two epicentral distances ($\Delta = 0.6°$ and 95.5°) are given. An 80 second time window centered around the arrival times of S and the CMB reflections, determined by ray theory, was extracted. Superimposition of the waveforms reveal travel time errors and numerical dispersion effects of these phases relative to S.

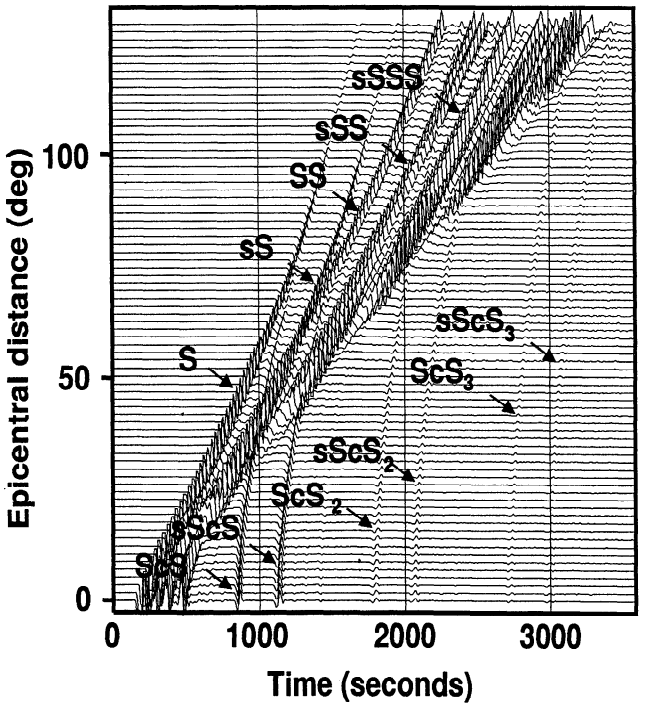

Figure 2. Seismograms for a source at 640km depth. The seismograms are one hour long. The maximum epicentral distance is 125°. Large amplitudes have been clipped. Some of the phases are marked (see also Figure 1). The 9 June 1994 deep earthquake under northern Bolivia produced excellent observations of these phases.

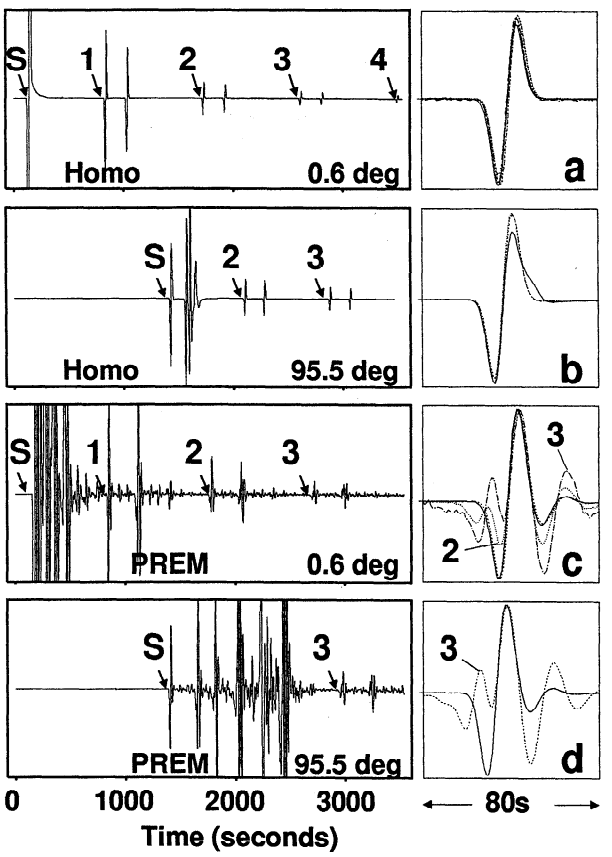

Figure 3. Left: Seismograms for different models and epicentral distances. The n-th CMB reflection is marked by n. **Right:** Normalized phases indicated on the left, aligned according to ray-theoretical travel times. If the waveforms deviate from each other they are marked. S is marked by a solid line. **a:** Homogeneous mantle, $\Delta = 0.6°$. **b:** Homogeneous mantle, $\Delta = 95.5°$. **c:** PREM, $\Delta = 0.6°$. **d:** PREM, $\Delta = 95.5°$.

In Figure 3a, the CMB reflections show only a slight error w.r.t. S in the relative amplitude of the wavelets. ScS_4 has propagated ≈140 wavelengths and the travel time error is ≈1 s, whereas the other phases have travel time errors smaller than 0.5 s. Note that with a second order scheme (same grid) the travel time error for ScS_4 is 4 s. In Figure 3b, the change in the waveform of the S-wave is caused by interference with ScS ($\Delta = 95.5°$). The travel time error for ScS_2 and ScS_3 is smaller than 0.5 s.

The same analysis is applied to seismograms obtained for PREM (same source parameters, Figures 3c,d). Due to interference from other signals, it is difficult to estimate dispersion effects. ScS_2 and ScS_3 wave forms are complicated by bottomside reflections from the crustal discontinuities at 15 and 24.4km depth in PREM. Note that ScS in Figure 3c shows an excellent fit to S since it does not have these precursors.

For all the superimposed waveforms, the travel time error, determined at the dominant peak, is below 1 s. While the waves recorded at $\Delta = 0.6°$ propagate mainly in a radial direction, the signals recorded at $\Delta = 95.5°$ propagate at various angles with respect to the grid. The results in Figure 3 suggest that the directional dependence of the dispersion effects are small. However, a more quantitative analysis will be desirable in the future.

Discussion and Conclusions

The main goal of this study was to investigate whether high-order FD approximations to the wave equation in spherical coordinates can be used to model broadband seismograms.

The main problems with the FD method are numerical dispersion and the computational effort required. Our results suggest that, with high-order approximations, it is possible to calculate global Earth synthetic SH-seismograms in frequency bands up to 0.1 Hz without significant dispersion of the wavetrain. However, small errors in the travel time exist, depending on the order of the scheme and the propagation length. Note that the spherical grid implies that the accuracy of the FD scheme is not only direction dependent (numerical anisotropy) but also space dependent (variable grid density with depth). In general, the scheme is less accurate near the Earth's surface due to the increasing horizontal grid spacing for smaller depths.

At present we are extending the method to the P-SV case, realistic sources (e.g. double couple), and media with attenuation.

In this study, we chose to simulate waves in two dimensions for models and wavefields invariant in φ. The reasons for this choice are that the 2D-approximation allows higher frequencies to be evaluated. In principle, 3D wave simulations in spherical coordinates are possible, but the complete wavefield, including all three displacement components, has to be considered. This will increase the memory requirements and therefore limit the frequency range that can be achieved.

In view of the developments in parallel hardware technology it is likely that the FD method will begin to play an important rôle for the simulation and inversion of generally heterogeneous global Earth structures.

Acknowledgments. Thanks to E. Chaljub for a preprint of their paper. We would also like to thank T. Dahm, M. Everett, R. Geller, F. Krüger, P. Mora and an anonymous reviewer for comments on this paper. We are grateful to the Centre National de Calcul Parallel en Science de la Terre (CNCPST) at the Institut de Physique du Globe de Paris for giving us access to the Connection Machine CM-5. One of the authors (HI) is funded by the Isaac Newton Trust.

References

Alterman, Z., J. Aboudi, and F.C. Karal, Pulse propagation in a laterally heterogeneous solid elastic sphere, *Geophys. J. R. Astron. Soc., 21*, 243-260, 1970.

Červený, V., M.M. Popov, and I. Pšenčik, Computation of wave-fields in inhomogeneous media – Gaussian beam approach, *Geophys. J. R. astr. Soc., 70*, 109-128, 1982.

Chaljub, E., A. Tarantola, and P. Shearer, Modeling SH-wave propagation in the Earth, *J. Geophys. Res., in press*, 1995.

Cummins, P.R., R.J. Geller, T. Hatori, and N. Takeuchi, DSM complete synthetic seismograms: SH, spherically symmetric case, *Geophys. Res. Lett., 21*, 533-536, 1994a.

Cummins, P.R., R.J. Geller, and N. Takeuchi, DSM complete synthetic seismograms: P-SV, spherically symmetric case, *Geophys. Res. Lett., 21*, 1663-1666, 1994b.

Dziewonski, A., and D.L. Anderson, Preliminary reference Earth model, *Phys. Earth Planet. Int., 25*, 297-356, 1981.

Fuchs, K, and G. Müller, Computation of synthetic seismograms with the reflectivity method and comparison with observations, *Geophys. J. R. astr. Soc., 23*, 417-433, 1971.

Geller, R.J., and T. Ohminato, Computation of synthetic seismograms and their partial derivatives for heterogeneous media with arbitrary natural boundary conditions using the Direct Solution Method, *Geophys. J. Int, 116*, 421-446, 1994.

Igel, H., P. Mora., and B. Riollet, Anisotropic wave propagation through FD grids, *Can. J. Expl. Geophys., 29*, 59-77, 1993.

Rodrigues, D., and P. Mora, Analysis of a finite-difference solution to the three-dimensional elastic wave-equation, *Expanded Abstracts, Society of Exploration Geophysics Meeting 1992*, 1247-1249, 1992.

Shearer, P.M., Imaging global body-wave phases by stacking long-period seismograms, *J. Geophys. Res., 96*, 20353-20364, 1991.

Virieux, J., P-SV wave propagation in heterogeneous media: velocity-stress finite-difference method, *Geophysics, 51*, 889-901, 1986.

Wysession, M.E., and P.J. Shore, Visualization of whole mantle propagation of seismic shear energy using normal mode summation, *Pure Appl. Geophys., 142*, 295-310, 1994.

Woodhouse J.H., and A.M. Dziewonski, Mapping the upper mantle: three-dimensional modeling of Earth structure by inversion of seismic waveforms, *J. Geophys. Res., 89*, 5953-5986, 1984.

Heiner Igel, Institute of Theoretical Geophysics, Department of Earth Sciences, University of Cambridge, Downing Street, Cambridge, CB2 3EQ, UK, heiner@esc.cam.ac.uk

Michael Weber, Institut für Geophysik, Universität Göttingen, Herzberger Landstr. 180, D – 37075 Göttingen, Germany, mhw@willi.uni-geophys.gwdg.de

(received November 4, 1994;
revised January 12, 1995;
accepted January 12, 1995.)